INSTITUTE OF PHYSICS PUBLISHING SEMICONDUCTOR SCIENCE AND TECHNOLOGY

Semicond. Sci. Technol. **20** (2005) 956–960 doi:10.1088/0268-1242/20/9/012

Influence of the kink effect on the dynamic performance of short-channel InAlAs/InGaAs high electron mobility transistors

B G Vasallo, J Mateos, D Pardo and T González

Departamento de Física Aplicada, Universidad de Salamanca, Plaza de la Merced s/n, 37008 Salamanca, Spain

E-mail: a50343@usal.es

Received 2 June 2005, in final form 5 July 2005
Published 1 August 2005
Online at stacks.iop.org/SST/20/956

Abstract

A semiclassical two-dimensional ensemble Monte Carlo simulator is used to perform a microscopic study of the influence of the kink effect on the dynamic behaviour of short-channel InAlAs/InGaAs lattice-matched high electron mobility transistors (HEMTs). To this end, the transient behaviour of the kink onset and the degradation introduced in some elements of the small signal equivalent circuit are analysed. According to our results, the pile-up of holes (generated by impact ionization) which is at the origin of the kink effect, jointly with the higher electron density in the channel, causes an increase of the gate–source capacitance. The drain conductance also increases because the accumulated hole density depends significantly on the drain–source voltage. In addition, the frequency dependence of the drain conductance reflects the influence of the hole recombination processes taking place in the accumulation zone.

1. Introduction

Although InP-based high electron mobility transistors (HEMTs) are the most promising candidates for active devices in high-speed and high-frequency integrated circuits, their utility for microwave power applications is limited when the kink effect (an anomalous increase in the drain current I_D at sufficiently high drain–source voltages V_{DS}) emerges, so that its analysis is considered to be essential for the development of these transistors [1–5]. In particular, this phenomenon leads to a large degradation in the dynamic performance of the HEMT [3, 6]. Remarkably, the drain conductance g_d presents experimentally a significant frequency dispersion, with an important increase of the low-frequency value [7–9]. To explain the kink phenomena and the associated enhancement of g_d, most authors refer to the analytical model of [3]. This model is based principally on a shift of the threshold voltage of the transistor caused by the presence of an accumulation of holes (generated by impact ionization) in the gate–source side of the channel. However, the explanation of the kink dynamics, specially the frequency behaviour of g_d, is still controversial, particularly for short-channel HEMTs.

As an alternative to this model, we present a microscopic study of the influence of the kink effect on the dynamic behaviour of InAlAs/InGaAs HEMTs performed by means of a 2D Monte Carlo (MC) simulator that incorporates all the processes at the basis of this phenomenon. In previous works, we have verified the origin of the kink effect in this type of HEMTs [10, 11]. These transistors are very susceptible to suffer impact ionization processes due to the small bandgap of InGaAs and the very high electric fields appearing in the gate–drain region when the device dimensions are shortened to improve the operation frequency. Holes generated by impact ionization tend to pile up under the source side of the gate due to the negative surface charge placed at the gate side of the recess and, mainly, to the negative gate voltage V_{GS}. This leads to a reduction in the potential barrier which controls the passage of electrons through the channel, which is further opened. As a consequence, I_D increases, causing the kink effect in the output characteristics. The total amount of accumulated holes depends strongly on the

hole recombination processes, which become very influential on the kink effect and, consequently, on its dynamics. The principal aim of the present work is to connect the origin of the kink effect to the degradation introduced on the dynamic performance of the HEMT. With this purpose, we study the transient performance of the kink onset and the behaviour of some relevant elements of the small signal equivalent circuit (SSEC).

This paper is organized as follows. In section 2 the physical model employed in the analysis is described. The main results and their discussion are provided in section 3. Finally, in section 4 the most important conclusions of this work are drawn.

2. Physical model

The device under study is a 100 nm T-gate recessed $In_{0.52}Al_{0.48}As/In_{0.53}Ga_{0.47}As$ HEMT, widely described in [12]. We employ an ensemble MC simulator self-consistently coupled with a 2D Poisson solver which incorporates all the processes at the origin of the kink effect, essentially impact ionization and hole recombination [10]. Electron impact ionization is implemented by using the Keldysh approach [13], with values of 0.8 eV for the ionization threshold energy E_{th} and 2×10^{12} s^{-1} for the parameter S which measures the softness or hardness of the threshold. Hole recombination is considered to take place with a characteristic time τ_{rec} (i.e., with a probability $1/\tau_{rec}$). The values employed in our study (between 0.01 and 0.1 ns) are slightly shorter than the real ones (about 1.0 ns [2, 3]), since τ_{rec} is the longest characteristic time among those involved in the system under analysis, and values of the order of ns would lead to extremely long simulation times [10].

As an initial step in the investigation of the dynamic performance of the HEMT, we analyse the transient behaviour of the kink onset. To this purpose, we perform calculations in which the steady-state conditions for $V_{DS} = 0$ are first attained, and then a high value of V_{DS} is applied (for which kink effect emerges). This analysis reflects what occurs experimentally when a voltage V_{DS} is applied starting from $V_{DS} = 0$ [3, 14]. The MC technique allows us to study the evolution of the drain current I_D with the simulation time, since it provides the instantaneous values of I_D [10].

As a second step, to characterize rigorously the dynamic behaviour of a transistor, the calculation of its small signal equivalent circuit (SSEC) is required. In our study, the elements of the small signal equivalent circuit are determined by means of the Y parameters, which connect, for each frequency f, the small-signal variations in the gate and the drain currents, $i_1(f)$ and $i_2(f)$, respectively, with the relative variations in the gate and drain voltages, $v_1(f)$ and $v_2(f)$, respectively. The general expression for $Y_{ij}(f)$ is

$$Y_{ij}(f) = \left(\frac{i_i(f)}{v_j(f)}\right)_{v_{i,i\neq j}=0}. \tag{1}$$

Y_{11} and Y_{22} are, respectively, the input and the output admittances, Y_{12} is the feedback admittance and Y_{21} is the transconductance. The Y parameters are usually calculated by means of the Fourier analysis of the transit response of the transistor to voltage steps applied at the gate and drain electrodes [15, 16]. In our case, the precision of this technique is not good enough due to the long characteristic times involved in the system under analysis. As an alternative, for a given stationary operation condition a sinusoidal voltage signal of frequency f is applied to the gate and drain electrodes (separately) and the response in the output currents is evaluated. Accordingly, a signal $v_1(t) = |v_1| \exp(\mathrm{j}2\pi f t)$ is applied to the gate (j being the imaginary unit), with a sufficiently low value for $|v_1|$ to assume a lineal response in the gate and drain currents, $i_1(t)$ and $i_2(t)$, respectively. The response currents are adjusted to sinusoidal signals with the same frequency f and a diphase φ, in the form $|i_1| \exp[\mathrm{j}(2\pi f t + \varphi_{11})]$ and $|i_2| \exp[\mathrm{j}(2\pi f t + \varphi_{21})]$, respectively. Then,

$$Y_{11} = i_1/v_1 = [|i_1|/|v_1|] \exp(\mathrm{j}\varphi_{11}) \tag{2}$$

and

$$Y_{21} = i_2/v_1 = [|i_2|/|v_1|] \exp(\mathrm{j}\varphi_{21}) \tag{3}$$

are calculated. Similarly, a signal $v_2(t) = |v_2| \exp(\mathrm{j}2\pi f t)$ is applied to the drain, with $|v_2|$ also low enough for a lineal response of the device. The adjusted currents in the gate and the drain are $|i_1| \exp[\mathrm{j}(2\pi f t + \varphi_{21})]$ and $|i_2| \exp[\mathrm{j}(2\pi f t + \varphi_{22})]$. Then,

$$Y_{12} = i_1/v_2 = [|i_1|/|v_2|] \exp(\mathrm{j}\varphi_{12}) \tag{4}$$

and

$$Y_{22} = i_2/v_2 = [|i_2|/|v_2|] \exp(\mathrm{j}\varphi_{22}) \tag{5}$$

are computed. This process is repeated for each required frequency. The elements of the SSEC of the HEMT [17, 18] are connected to the Y parameters through the expressions given in [17, 19]. These elements have been widely analysed for low V_{DS}, i.e., in the absence of impact ionization [18, 20]. We are specially interested in the study of the elements of the SSEC more susceptible to the influence of the kink effect: the gate–source capacitance C_{gs}, the transconductance g_{m0} and the output conductance g_d.

3. Results

As a first approximation to the study of the kink effect dynamics, we analyse the transient behaviour of the kink onset. We perform calculations in which steady-state conditions for $V_{DS} = 0$ (when impact ionization does not take place) are first attained, and then a high value of V_{DS} is applied at a time $t_{sim} = 0$, t_{sim} being the time elapsed after the onset of V_{DS}. Figure 1 shows the output characteristic corresponding to $V_{GS} = -0.3$ V at different t_{sim} for (*a*) $\tau_{rec} = 0.01$ ns, (*b*) $\tau_{rec} = 0.1$ ns and (*c*) $\tau_{rec} = 1.0$ ns. The case of absence of impact ionization and the values taken by I_D in the final steady state ($t_{sim} = t_{final}$) are plotted for comparison. For $t_{sim} = 0.05$ ns and $t_{sim} = 0.10$ ns, the pile-up of holes is completely formed only when considering $\tau_{rec} = 0.01$ ns. The steady-state value of I_D is observed to be reached for longer values of t_{sim} the higher τ_{rec} is, since the holes remain longer in the device without disappearing by recombination. Thus, the stationary value of the pile-up is higher and it is established later, which leads to a more pronounced kink effect (higher steady-state value of I_D). These results indicate that the kink effect is a low-frequency phenomenon, since

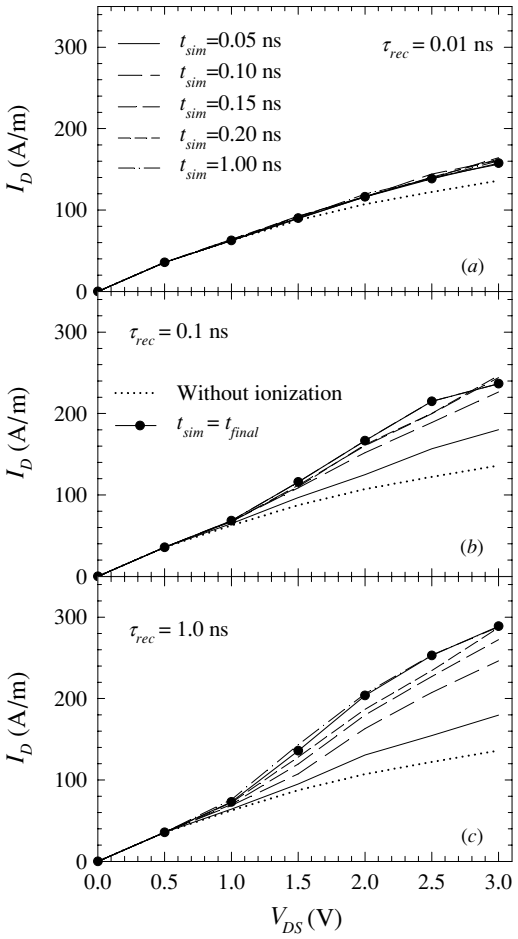

Figure 1. HEMT output characteristics at several simulation times $t_{\rm sim}$ from the onset of $V_{\rm DS}$ (starting from the equilibrium conditions, $V_{\rm DS} = 0$) for $V_{\rm GS} = -0.3$ V and different values of $\tau_{\rm rec}$ (*a*) 0.01 ns, (*b*) 0.1 ns and (*c*) 1.0 ns.

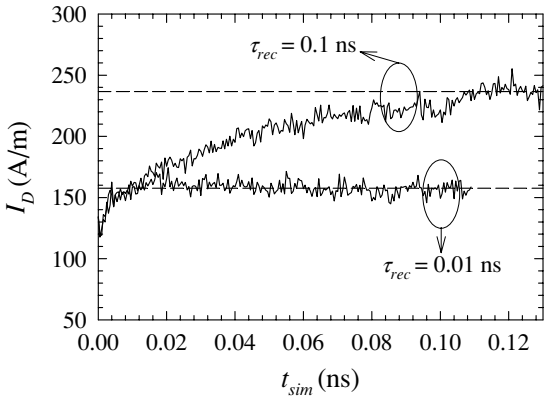

Figure 2. $I_{\rm D}$ versus $t_{\rm sim}$ elapsed since $V_{\rm DS} = 3.0$ V is applied at $t_{\rm sim} = 0$ (starting from the equilibrium conditions, $V_{\rm DS} = 0$) for $V_{\rm GS} = -0.3$ V and different $\tau_{\rm rec}$. The dash lines show the mean value of $I_{\rm D}$ in the final steady-state condition.

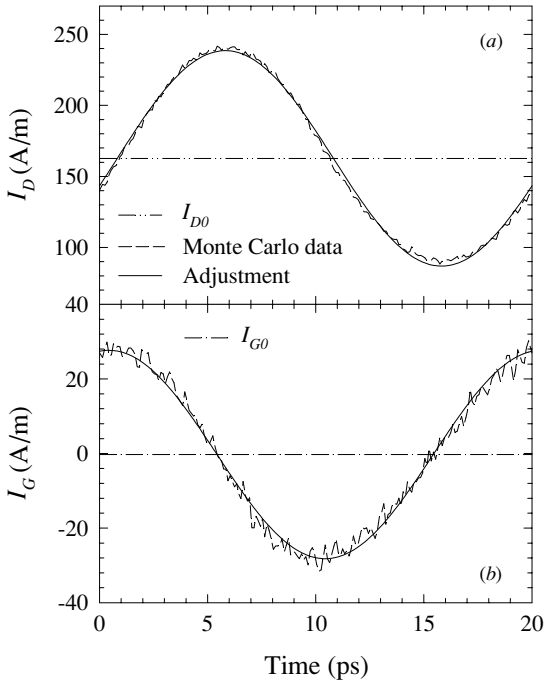

Figure 3. (*a*) $I_{\rm G}$ and (*b*) $I_{\rm D}$ responses to a sinusoidal signal $v_{\rm G}(t) = |v_{\rm G}|\exp(\mathrm{j}2\pi f t)$ with $|v_{\rm G}| = 0.15$ V and $f = 50$ GHz applied to the gate electrode for $V_{\rm GS} = -0.3$ V and $V_{\rm DS} = 3.0$ V to compute the Y parameters. $\tau_{\rm rec} = 0.01$ ns is considered.

long times are required to establish the accumulation of holes (compared to the typical values of other characteristic times of the HEMT). The drain–current evolution as a function of the simulation time $t_{\rm sim}$ in this numerical experiment is plotted in figure 2 for two different recombination times, $\tau_{\rm rec} = 0.01$ ns and $\tau_{\rm rec} = 0.1$ ns, when $V_{\rm GS} = -0.3$ V and $V_{\rm DS}$ becomes 3.0 V from 0 V at the time $t_{\rm sim} = 0$. The dashed lines indicate the mean value of $I_{\rm D}$ at $t_{\rm final}$. As observed, the time necessary to reach the final steady state is of the order of $\tau_{\rm rec}$, which is, subsequently, the most important characteristic time among those involved in the system evolution. Remarkably, these results are in good qualitative agreement with the experimental measurements presented in [3, 14].

The influence of the kink on the dynamic behaviour can be more rigorously studied considering the SSEC representation. As mentioned in section 2, the Y parameters are computed by applying a sinusoidal signal of frequency f to the gate and drain electrodes and evaluating the response in the output currents, which are then adjusted to sinusoidal signals of the same frequency. We present the following example to picture this procedure. To obtain Y_{11} and Y_{21} for 50 GHz, a signal $v_1(t) = |v_1|\exp(\mathrm{j}2\pi f t)$ with $|v_1| = 0.15$ V and $f = 50$ GHz is applied to the gate electrode, being the stationary point $V_{\rm GS} = -0.3$ V, $V_{\rm DS} = 3.0$ V. Figure 3 shows the output currents (*a*) $I_{\rm D}(t) = I_{\rm D0} + i_2(t)$ and (*b*) $I_{\rm G}(t) = I_{\rm G0} + i_1(t)$, as well as the adjusted sinusoidal signals with frequency 50 GHz. For instance, the amplitude and the diphase obtained for $i_2(t)$ are $|i_2| = 75.8\ \mathrm{A\,m^{-1}}$ and $|\varphi_{12}| = -0.456\pi$ rad, respectively. From the relations i_1/v_1 and i_2/v_1 the real and imaginary parts of Y_{11} and Y_{21} are obtained for $f = 50$ GHz. Similarly, a sinusoidal signal $v_2(t) = |v_2|\exp(\mathrm{j}2\pi f t)$ with $|v_2| = 0.5$ V and $f = 50$ GHz is applied in the drain electrode to obtain Y_{12} and Y_{22}. The procedure is similar for each required frequency. In figure 4 the resulting values of (*a*) Y_{11}, Y_{21} and (*b*) Y_{12}, Y_{22} are presented as functions of f for

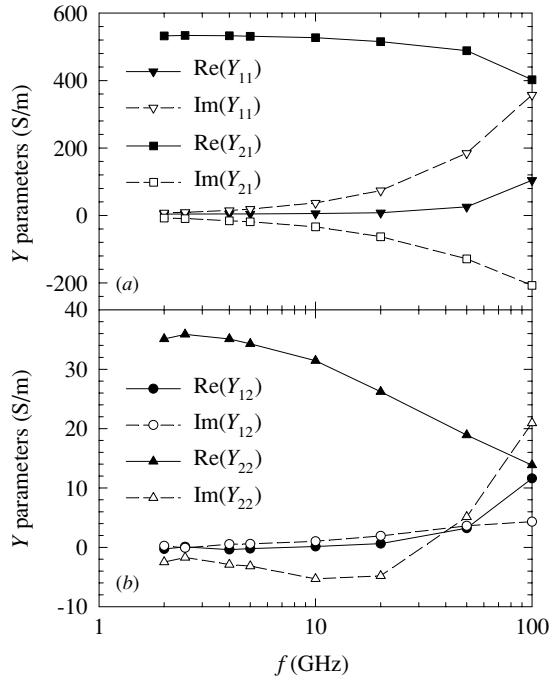

Figure 4. (*a*) Y_{11}, Y_{21} and (*b*) Y_{12}, Y_{22} as a function of frequency for $V_{GS} = -0.3$ V and $V_{DS} = 3.0$ V. $\tau_{rec} = 0.01$ ns is considered.

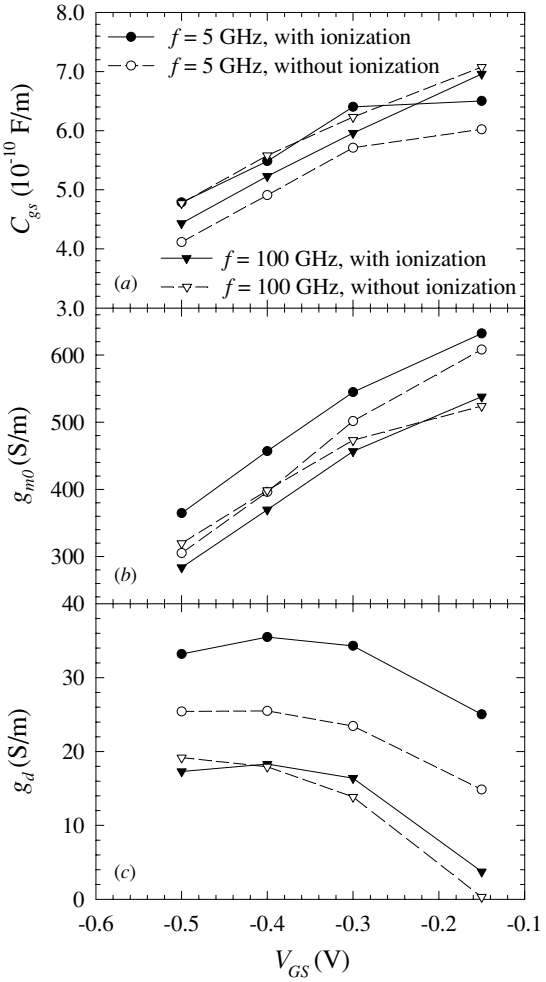

Figure 5. (*a*) C_{gs}, (*b*) g_{m0} and (*c*) g_d versus V_{GS} for different frequencies f when $V_{DS} = 3.0$ V and $\tau_{rec} = 0.01$ ns. The corresponding cases of absence of impact ionization are plotted for comparison.

$V_{GS} = -0.3$ V, $V_{DS} = 3.0$ V and $\tau_{rec} = 0.01$ ns. The real and imaginary parts of the input admittance Y_{11} grow with frequency, the imaginary part being higher (associated with the gate capacitance). The transconductance Y_{21} is practically real at low frequencies, but its imaginary part increases with f. The feedback admittance Y_{12} is practically null up to very high frequencies. The real part of the output admittance Y_{22} is the drain conductance, g_d, which will be analysed later.

As indicated in section 2, we are interested in the elements of the SSEC more susceptible to the influence of impact ionization. Figure 5 shows for 5 and 100 GHz (*a*) the gate–source capacitance C_{gs}, (*b*) the transconductance g_{m0} and (*c*) the drain conductance g_d, as functions of V_{GS}, for $V_{DS} = 3.0$ V and $\tau_{rec} = 0.01$ ns. The corresponding cases of absence of impact ionization are also sketched for comparison. The dependence of C_{gs}, g_{m0} and g_d on V_{GS} is the same in both situations, with and without impact ionization in the simulated structure (increase of C_{gs} and g_{m0}, and decrease of g_d, as V_{GS} increases). The onset of impact ionization processes leads to an enlargement of all of these elements for 5 GHz. According to our results, the increase of C_{gs} is caused by the pile-up of positive charge in the channel between the gate and the source, which leads to a higher electron density in the drain side of the channel. g_{m0} also increases with the onset of the kink, indicating that a change of V_{GS} provokes a stronger modification in I_D than in the absence of impact ionization processes, due to the variations of the accumulated positive charge. g_d is the parameter most affected by the presence of the kink effect. Its enhancement indicates that the variations of I_D caused by a modification of V_{DS} are amplified by the response of the hole pile-up in the channel, more strongly for larger V_{DS} [10]. When the operation frequency becomes higher, the relative enhancement of these parameters with respect to the case of absence of impact ionization is less significant. In particular, at 100 GHz the positive charge accumulated in the channel hardly responds to the input signal variations and, thus, the differences of C_{gs}, g_{m0} and g_d when compared to the values obtained without ionization are much smaller. The only influence that can be observed is the change of the static operating conditions (V_{GS} shift) due to the accumulation of holes.

g_d is the element of the SSEC which can give more information about the modifications introduced by the kink effect in the dynamic behaviour of the HEMT. Figure 6 shows g_d as a function of frequency for $V_{GS} = -0.3$ V, $V_{DS} = 3.0$ V and two different values of τ_{rec}, 0.1 and 0.01ns. The case of absence of impact ionization is also sketched for comparison. As observed, the value reached by g_d at low frequency is higher for the longer τ_{rec} considered (since the kink effect is more significant [10]). Moreover, the low-frequency contribution of g_d exhibits a cutoff frequency of the order of $1/\tau_{rec}$, which is clearly related to the presence of the kink effect. Other times could affect the cutoff frequency: the characteristic time of impact ionization and the time which holes take to move from the region where

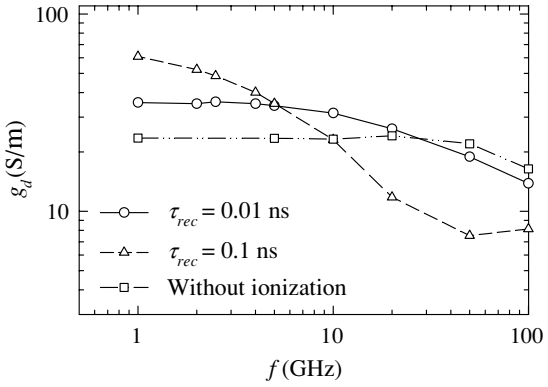

Figure 6. g_d versus frequency for different τ_{rec} when $V_{GS} = -0.3$ V and $V_{DS} = 3.0$ V. The corresponding case of absence of impact ionization is plotted for comparison.

they are generated to the accumulation zone. These times are difficult to determine. However, following the results of our simulations, we conclude that the most relevant time is τ_{rec}. Thus, the frequency dependence of the kink-related increase of g_d is governed by the time necessary for the setting up of the hole accumulation. The frequency dispersion obtained for g_d by our model has been observed experimentally in a 0.13μm InAlAs/InGaAs HEMT in the presence of the kink [7], as well as in a pseudomorphic HEMT with $In_{0.35}Ga_{0.65}As$ channel [8].

4. Conclusions

We have presented an MC-based study of the degradation introduced by the kink effect in the dynamic performance of a short-channel lattice matched $In_{0.52}Al_{0.48}As/In_{0.53}Ga_{0.47}As$ HEMT. With this purpose, we have analysed the transient behaviour of the kink onset and the kink influence on the SSEC elements most susceptible to be deteriorated. According to our results, the most relevant characteristic time amongst those involved in the system evolution is τ_{rec}, which is the time necessary to set up the hole accumulation in the channel (which causes the appearance of the kink effect). The dynamic behaviour of the HEMT is strongly degraded by the kink onset mainly due to the increase of C_{gs} and g_d. The frequency dependence of g_d is related to the dynamics of the processes leading to the appearance of the kink effect.

Acknowledgments

This work has been partially supported by the Dirección General de Investigación (Ministerio de Educación y Ciencia) and FEDER through the project TEC2004-05231.

References

[1] Wada O and Hasegawa H 1999 *InP-Based Materials and Devices. Physics and Technology* (New York: Wiley)
[2] Suemitsu T, Enoki T, Sano N, Tomizawa M and Ishii Y 1998 *IEEE Trans. Electron Devices* **45** 2390
[3] Somerville M H, Ernst A and del Alamo J A 2000 *IEEE Trans. Electron Devices* **47** 922
[4] Di Carlo A, Rossi L, Lugli P, Zandler G, Meneghesso G, Jackson M and Zanoni E 2000 *IEEE Electron Device Lett.* **21** 149
[5] Sleimann A, Di Carlo A, Lugli P and Zandler G 2001 *IEEE Trans. Electron Devices* **48** 2188
[6] Parker A E and Rathmell J G 2001 *IEEE Trans. Microw. Theory Tech.* **49** 2105
[7] Arai T, Sawada K, Okamoto N, Makiyama K, Takahashi T and Hara N 2003 *IEEE Trans. Electron Devices* **50** 1189
[8] Hara N, Okamoto N, Imanishi K, Sawada K, Takahashi T, Makiyama K and Takikawa M 2004 *Proc. 16th Int. Conf. Indium Phosphide and Related Materials, IEEE Catalog 04CH37589* 615
[9] Pierobon R, Rampazzo F, De Pellegrin T, Bertazo M, Meneghesso G, Zanoni E, Suemitsu T and Enoki T 2004 *Proc. 16th Int. Conf. Indium Phosphide and Related Materials, IEEE Catalog 04CH37589* 623
[10] Vasallo B G, Mateos J, Pardo D and González T 2003 *J. Appl. Phys.* **94** 4096
[11] Vasallo B G, Mateos J, Pardo D and González T 2004 *J. Appl. Phys* **95** 8271
[12] Mateos J, González T, Pardo D, Hoël V and Cappy A 2000 *IEEE Trans. Electron Devices* **47** 1950
[13] Fischetti M V 1991 *IEEE Trans. Electron Devices* **38** 634
[14] Ernst A N, Somerville M H and delAlamo A 1997 *IEEE Electron Device Lett.* **18** 613
[15] Moglestue C 1993 *Monte Carlo Simulation of Semiconductor Devices* (London: Chapman and Hall)
[16] Tomizawa K 1993 *Numerical Simulation of Submicron Semiconductor Devices* (Boston: MA: Artech House)
[17] González T, Pardo D, Varani L and Reggiani L 1995 *IEEE Trans. Electron Devices* **42** 991
[18] Mateos J, González T, Pardo D, Hoël V, Happy H and Cappy A 2000 *IEEE Trans. Electron Devices* **47** 250
[19] Dambrine G, Cappy A, Heliodore F and Playez E 1988 *IEEE Trans. Microw. Theory Tech.* **32** 1151
[20] Mateos J, González T, Pardo D, Hoël V and Cappy A 1999 *Semicond. Sci. Technol.* **14** 864